A microstructural examination of apatite induced by Bioglass® *in vitro*

J. P. ZHONG, D. C. GREENSPAN
US Biomaterials Corporation, One Progress Blvd. #23, Alachua, FL, USA
J. W. FENG
Shanghai Institute of Ceramics, Chinese Academy of Science, 1295 Dingxi Road, Shanghai, 200050, P.R. China

Bioglass®, a clinically used bone graft material, has been tested *in vitro* in a simulated body fluid (SBF) up to four weeks. Apatite crystals were not only found to form on its surface but also in the reaction solutions. The apatite crystals have been examined by high-resolution transmission electron microscopy (TEM). The crystals formed in the solutions appear identical in morphology and structure with those formed on the Bioglass® surface. It may be that the soluble Si in the solution serves as the nucleating site for the apatite crystal or that apatite nuclei are released from the Bioglass® surface to the solution resulting in crystal growth.

Introduction

Since Hench initiated work on bioactive glasses [1] in 1970, many bioactive ceramics have been investigated worldwide including bioactive glasses [1–3], gels [4–6] and glass–ceramics [7]. The term ''bioactive'' relates to the ability of a synthetic material to form a chemical bond with bone or soft tissue [8, 9]. During the past 10 years, the clinical success of Bioglass® as a bone graft material has been attributed to its rapid bonding to living tissue and stimulation of bone growth [8]. It has been well recognized that this biological behavior is always associated with the formation of a hydroxy-carbonate apatite (HCA) on the Bioglass® surface [8, 10]. This HCA layer has been shown to result from the surface reactivity of the glass.

The formation of hydroxyapatite (HA) and other calcium phosphate species from solutions saturated with calcium and phosphate has been well known and studied for many years [11–13]. The nucleation in this chemical process is homogenous. However, the nucleation of HA on Bioglass® is heterogeneous. When Bioglass® is exposed to a physiological solution a specific sequence of surface reactions will occur [14]. The rates and extent of these reactions depend on the exact make-up of the solutions, and the ratio of exposed surface area to solution volume [15, 16]. In general, the first reaction is the exchange of Na^+ and other modifying cations in the glass with H^+ and H_3O^+ in solution, allowing a breakdown of Si–O–Si bonds. This results in Si–OH groups that will repolymerize to form a silica-rich layer on the surface. This is followed by the formation of an amorphous calcium phosphate film on the silica-rich layer. Eventually the crystallization of the amorphous CaP leads to the HCA formation. The mechanism for the nucleation and growth of these calcium-based phases on Bioglass® is still not quite clear, but a number of hypotheses have been proposed in many publications.

In 1987, Walker [15] and later Greenspan *et al*. [16] demonstrated that only those bioactive glasses which developed high surface area (larger than 40–80 m^2/g) in a physiological environment could induce HCA formation. In many other publications on bioactive glasses and gel glasses, silica gel and bioactive glass-ceramics [4–6, 17–19], it has been shown that the high surface area provides a high concentration of surface silanol groups ($\equiv$ Si–OH) that serve as nucleation sites for the crystallization of HCA. Karlsson has proposed that the silanol groups on the gel layer are flexible enough to supply the correct atomic distances required by the crystal structure of HCA [20]. Meanwhile, work by Li and colleagues [21] concluded that the combination of a large number of hydroxyl groups and negative charges on the bioactive gel surface were necessary for the induction of HCA. They demonstrated that the negative charge would accumulate cations such as Ca^{2+} on the surface and would ultimately lead to precipitation of calcium phosphate. This hypothesis successfully predicted that SiO_2 and TiO_2 gels with a negative surface charge would induce HCA in a simulated body fluid (SBF) while Al_2O_3 gel with a positive surface charge would not [22]. Experiments conducted by one of the current authors also demonstrated that even a small amount of $Al^{3+}(2 \times 10^{-4}\,M)$ in solution would convert the negative charge on a silica gel surface to positive and eventually retard HCA formation [23]. The common feature in all of the studies is that the silanol groups of the bioactive silicas and the TiOH groups of TiO_2 are critical for the formation of the biological apatite in the

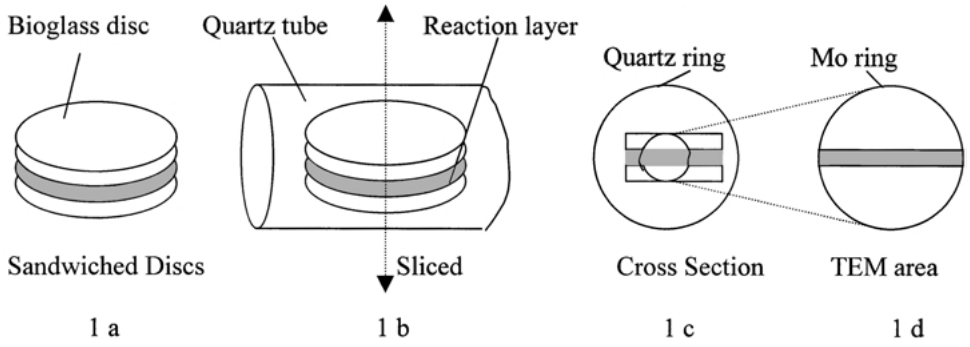

Figure 1 Diagram of TEM sample preparation.

physiological environment due to the negative surface charge.

Recently, Hench proposed that the soluble silicon from Bioglass® released to the surrounding tissue in conjunction with the HCA formation would promote bone production [24]. He has postulated that the soluble Si from bioactive glass activated bone stem cells to produce growth factors which adsorb on the silica gel and HCA led to rapid proliferation of bone cells, and mineralization of osteoid at the interface leading to a bond of glass to bone. A recent *in vivo* work has confirmed that silicon has been found even in a remote area (2 mm) away from the implant site and this region was found to be actively forming bone tissue by endochondral formation [25]. From above work, it is still not clear whether the microcrystals of HCA formed on the Bioglass® are released to the surrounding tissue as the silica glass network breaks down, or if the release of soluble silica is responsible for nucleating HCA formation directly from the surrounding tissue.

This paper will report our recent *in vitro* work on Bioglass®. The apatite formed on Bioglass® and in solution *in vitro* has been characterized by FTIR, examined by SEM and TEM. The data may provide some answers to above questions.

Materials and methods

45S5 Bioglass® disks and powders were reacted in tris buffer or a simulated body fluid (SBF). Tris buffer is a simple organic buffer solution and SBF contains ionic concentration similar to human blood plasma [26]. The composition and preparation of 45S5 Bioglass® has been described in detail in literature [27]. Briefly, reagent grade oxides (45% SiO_2, 24.5% CaO, 24.5% Na_2O and 6% P_2O_5) are mixed and melted at 1350 °C for 4 h to allow homogeneity of the melt and then, quenched to create frit. The glass powders were attained by ball milling of the frit followed by sieving. Disks were cast in graphite modes by re-melting the frit.

Bioglass® disks were reacted in tris buffer by suspending them in the solution at 37 °C with the ratio of surface area to solution volume (SA/V) of 0.1 cm^{-1}. The discs were withdrawn from the solution at 1, 3 and 7 day time periods, and dried with acetone. The samples were then ready for characterization.

The *in vitro* tests for powders in both tris buffer and the SBF were conducted dynamically in an orbital shaker at 175 rpm and 37 °C for time periods from 1, 3, 6 h and 1, 7, 14 and 28 days. The SBF without powders was also reacted along with those tests to verify if any precipitation would occur in the solution since it contains significant concentrations of ions. The dynamic test allows for uniform exposure of the particles to the test solution, thereby generating a homogenous reaction. The ratio of surface area to solution volume (SA/V) in this dynamic test was 0.4 cm^{-1}. As has been reported previously, this ratio in the dynamic test procedure generates the optimal reaction on the particle surface [28]. The solutions were exchanged at time intervals of 6 and 24 h and then every two days to prevent saturation of the solution. The samples were recovered using vacuum filtration with 5 μm filter paper and then rinsed by acetone to prevent further surface reaction. Particulate samples were then ready for surface analysis.

Apatite crystal morphology was examined by SEM and the structure examined by TEM. The diagram of the sample preparation for TEM can be seen in Fig. 1. The sample for TEM examination was prepared as follow: two reacted Bioglass® disks were sandwiched together by epoxy resin (Fig. 1a). After the epoxy cured, the sandwiched sample was placed perpendicularly into a quartz tube and cemented again with epoxy resin (Fig. 1b). The sample was sliced along the cross-section carefully to protect the crystal layer (Fig. 1b). The sliced sample surrounded by the epoxy resin and quartz ring was polished to thickness of 40 μm (Fig. 1c). The quartz

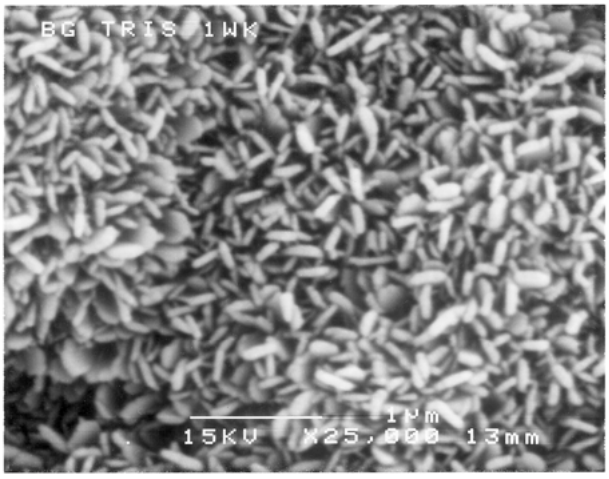

Figure 2 SEM morphology of apatite on Bioglass® reacted in tris for one week.

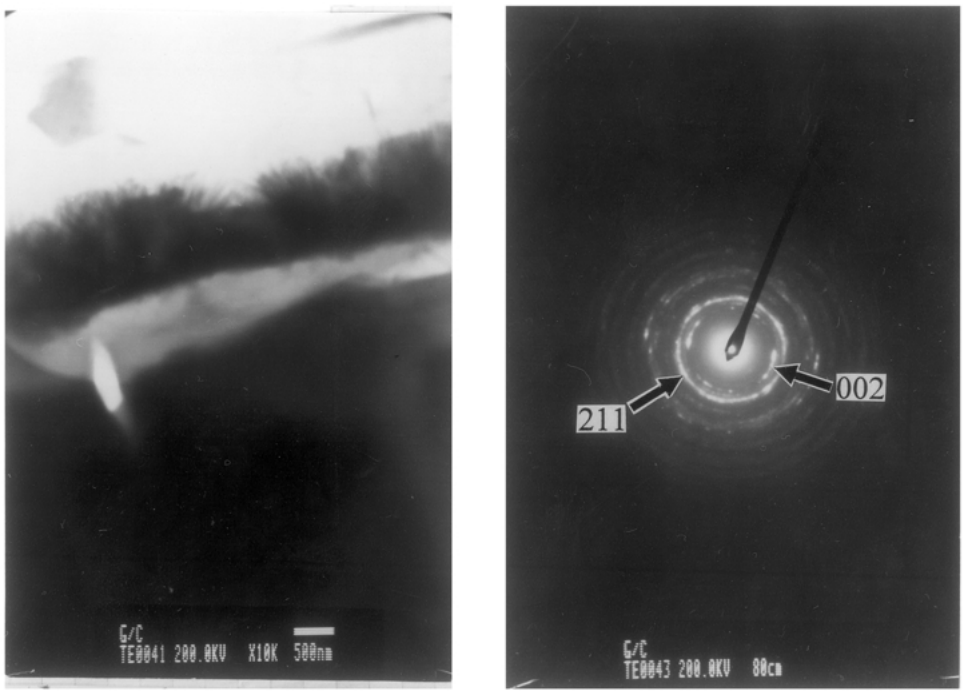

Figure 3 TEM and electron diffraction of apatite on Bioglass® reacted in tris for one week.

ring and the epoxy resin around the sliced sample would keep the two parts of the sample from separation during polishing. After polishing, a Mo ring (∅3 mm) was pasted on to the center of the sample film with epoxy. The part of the sample outside the Mo ring was removed by a scalpel (Fig. 1d). This sample underwent a further thinning by ion beam bombardment. Then, the sample was coated with carbon and ready for TEM examination.

Results

Fig. 2 is a SEM micrograph of the apatite crystals formed on the Bioglass® surface in tris buffer after one week in solution. The flake-like crystals showed a typical morphology and average size of 0.5 μm. Fig. 3 is a TEM micrograph of the cross-section of a Bioglass® disk, which has also been reacted in tris for a week. The electron diffraction pattern of the crystal layer in Fig. 3 exhibits the (0 0 2) and (2 1 1) crystal planes of an apatite crystal. The EDX analysis of the TEM cross-section in Fig. 4 shows the Bioglass® substrate in the bottom, the silica gel layer in the middle, with the apatite crystals on top. The thickness of the apatite crystal layer is around 1 μm.

In the *in vitro* dynamic tests in SBF for Bioglass® powders, flake-like crystals appeared in the solutions after 14 days and grew in number and size. These crystals reached a volume greater than the starting Bioglass® powders after 28 days. The morphology of these crystals is shown in Fig. 5. The crystal structure has been examined under TEM in Fig. 6, clearly indicating that the needle-like micro-crystals weave together to form the flake-like crystals. The average width of the crystallites is 20 nm. The electron diffraction patten is shown in Fig. 6, and appears similar to the morphology in Fig. 2. The FTIR spectrum in Fig. 7 shows that the crystal is apatite

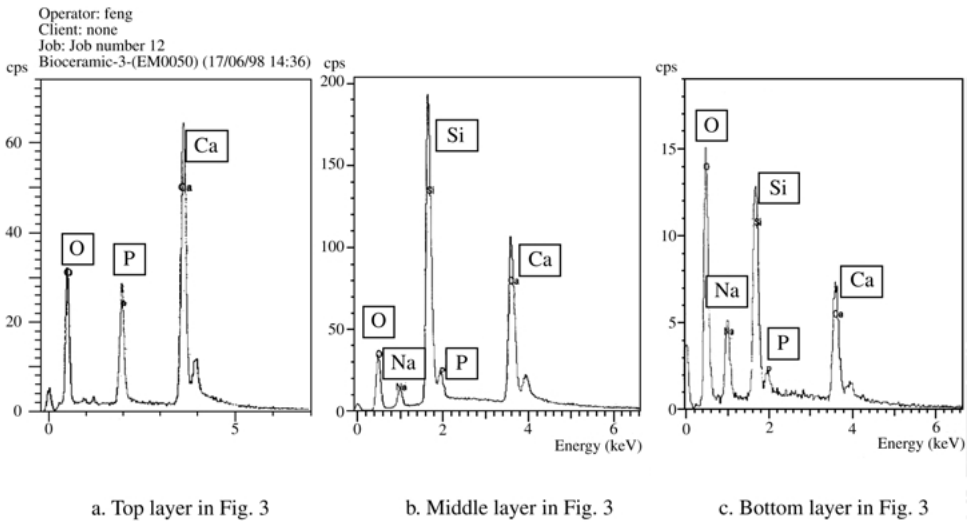

a. Top layer in Fig. 3 b. Middle layer in Fig. 3 c. Bottom layer in Fig. 3

Figure 4 EDX analysis of cross-section of Fig. 3.

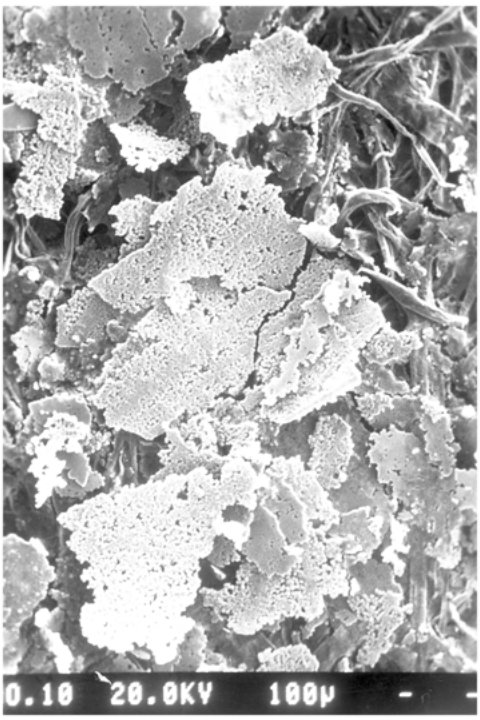

Figure 5 SEM morphology of apatite formed in reaction solutions.

indicated by the PO peak at around $1020\,cm^{-1}$ and the double peaks at $564\,cm^{-1}$ and $602\,cm^{-1}$.

Discussion

Apatite formed on Bioglass® surface

It has been well documented that apatite crystals form on Bioglass® when it is reacted in physiological solutions such as tris buffer, SBF, PBS and in cell culture medium [27, 29–31]. It has also been well recognized that the biological response of Bioglass® *in vivo* is always associated with the formation of the apatite crystals. The high surface area, pore structure, and formation of silanol groups with negative charges all contribute to the formation of the apatite layer.

In many previous publications, the apatite crystals formed on bioactive glasses were found to be either plate-like or needle-like [18, 31]. Plate-like crystals were mainly found in this work as shown in the SEM micrographs in Fig. 1. The cross-section of the apatite layer observed under TEM, demonstrated a crystal layer around 1 µm in thickness growing on the silica gel layer. Both FTIR spectra and electron diffraction patterns of the layer indicate that these are apatite crystals [32, 33]. Notably, the diffraction ring consists of some discontinuous diffraction spots in Fig. 2, which indicates that the apatite has undergone oriented growth on surface. Also, the SEM and TEM micrographs show the evidence of the oriented growth in which the crystals grow standing on the surface either vertically or at certain angles.

Apatite formed in solution

The apatite can be formed by precipitation from solutions that are saturated with calcium and phosphate. However, the experiments performed in this work demonstrate that there is no spontaneous precipitation of apatite crystals in SBF without Bioglass®. It is clear that the presence and reaction of Bioglass® initiates the apatite formation in SBF solution.

It has been reported in a previous publication that silicon is rapidly released from Bioglass® into the test solutions [34]. The silanol groups presenting on the soluble silica are the same as on the reacted Bioglass® surface. It is likely that the soluble Si could serve as a heterogeneous nucleation site to induce the apatite formation in the solution. This silica-induced apatite

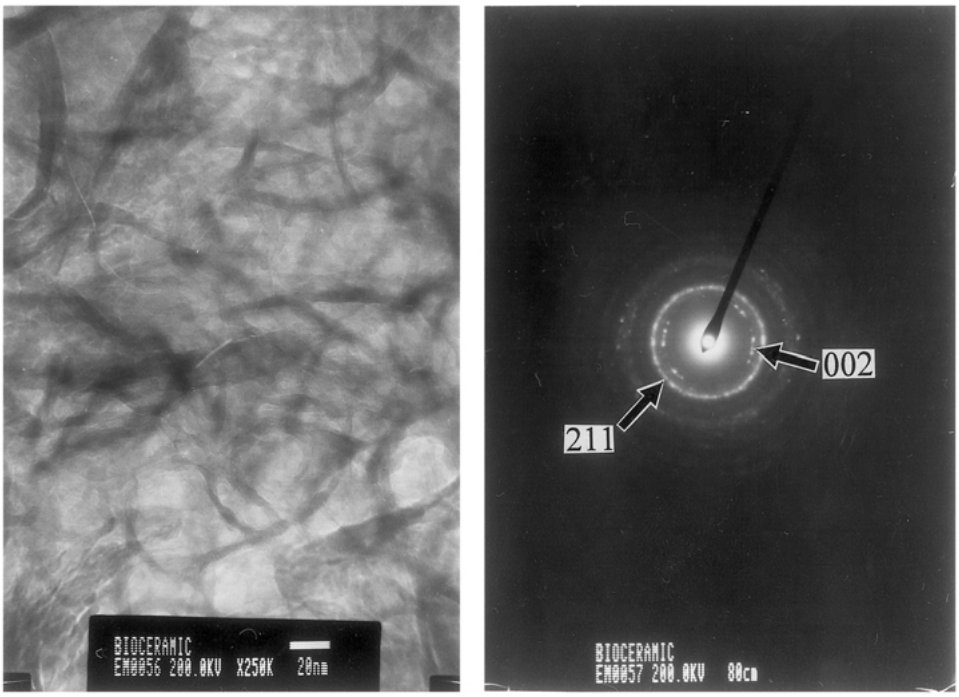

Figure 6 TEM and electron diffraction of apatite formed in reaction solution.

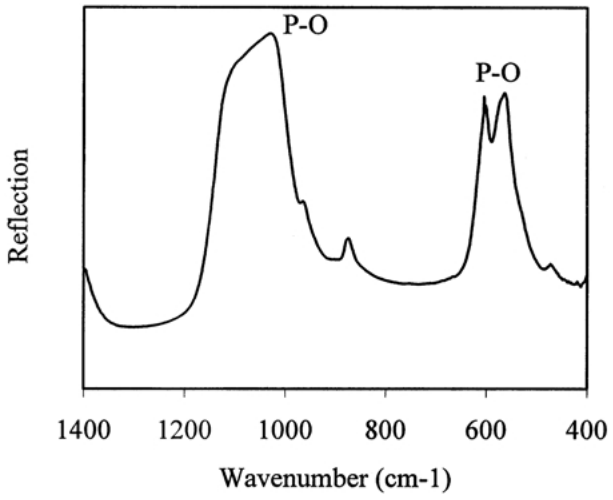

Figure 7 FTIR reflection spectrum of apatite formed in reaction solution.

formation is coincident with the silica-induced precipitation of calcium phosphate, which was reported by Damen and Cate [35, 36]. In their experiments, they found that calcium phosphate precipitation was caused by the introduction of silicic acid ($Si(OH)_4$) into calcium phosphate solutions. An alternative explaination for the apatite formation in the solution in this work is that the apatite nuclei form on the Bioglass® surface first and then leave the Bioglass® surface into solution, gradually growing to crystals.

As is shown in Fig. 5, the needle-like crystals formed from the solutions are around 5 nm in width and 20–80 nm in length, which are similar to the natural bone mineral phase both in shape and size [37]. In correlation with previously reported *in vivo* studies, this finding provides a clue that the silica-induced apatite formation could occur in the surrounding fluid and tissue after implantation. In a recent *in vivo* study, Chou found [25] that silicon presented in surrounding tissue, even in a remote area (2 mm away) from the Bioglass® implant site, where active mineralization and bone formation were found. Wilson had previously proposed a phenomenon she described as bone formation in the surrounding tissue remote from osteoconductive bone growth normally seen [38]. She termed this process as ''osteoproduction''. The mechanism Wilson described appears to be the same as that observed in Chou's study, and the work presented here is a plausible mechanism for explaining this phenomenon.

Conclusion

The formation of apatite crystals has been found in SBF by the presence and reaction of Bioglass®. The flake-like crystal consists of individual needle-like crystals which are identical in structure with the HA crystals formed on Bioglass® surface. It can be anticipated from this *in vitro* study that the implanted Bioglass®, in addition to its reactivity at the implant-tissue interface to enhance the bone bonding, also induces the formation of HA crystals in the surrounding tissue to participate in and stimulate bone growth. Future work should include short term *in vivo* studies to observe the formation of HCA microcrystals in surrounding tissue.

References

1. L. L. HENCH, R. J. SPLINTER, W. C. ALLEN and T. K. GREENLEE, *J. Biomed. Mater. Res. Symp.* **2**(1) (1972) 117.
2. M. OGINO, F. OHUCHI and L. L. HENCH, *J. Biomed. Mater. Res.* **14** (1980) 55.
3. C. Y. KIM, A. E. CLARK and L. L. HENCH, *J. Non-Cryst. Solids* **113** (1989) 195.
4. P. J. LI, X. Y. I. KANGASNIEMI, J. M. A. DE BLIECK-HOGERVORST, C. P. A. T. KLEIN and K. DE GROOT, *J. Biomed. Mater. Res.* **29** (1995) 325.
5. R. LI, A. E. CLARK and L. L. HENCH, *J. Appl. Biomater.* **2** (1991) 231.
6. M. M. PEREIRA, A. E. CLARK and L. L. HENCH, *J. Mater. Synth. and Proc.* **2**(3) (1994) 189–196.
7. T. KOKUBO, *Biomaterials* **12**(3) (1991) 155.
8. L. L. HENCH, *J. Am. Ceram. Soc.* **74**(7) (1991) 1487.
9. J. WILSON and D. NOLLETTI, in *Handbook of Bioactive Ceramics*, vol. 1, edited by T. Yamamuro, L. L. Hench and J. Wilson (CRC Press, Boca Raton, FL, 1990) p. 283.
10. Ö. H. ANDERSSON, K. H. KARLSSON and K. KANGASNIEMIA, *J. Non-Cryst. Solids* **121** (1990) 290.
11. A. L. BOSKEY and A. S. POSNER, *J. Phys. Chem.* **80**(1) (1976) 40.
12. E. D. EANES and A. S. POSNER, *Mater. Res. Bull.* **5** (1970) 377.
13. R. Z. LEGEROS, *Calcium Phosphates in Oral Biology and Medicine*, Karger, (1991).
14. L. L. HENCH, in ''Bioceramics 3'', edited by J. Hulbert and S. Hulbert (Rose-Hulman Institute of Technology, Terre Haute, India, 1991) p. 46.
15. M. M. WALKER, Master thesis, University of Florida (1977).
16. D. C. GREENSPAN, J. P. ZHONG and G. P. LATORRE, in ''Bioceramics 8'', edited by L. L. Hench, J. Wilson, and D. C. Greenspan (Elsevier Science, 1995) p. 477.
17. T. KOKUBO, S. B. CHO and K. NAKANISHI *et al.*, in ''Bioceramics 7'', edited by Andersson, Happonen, YliUrpo (Butterworth-Heinemann, 1994) p. 49.
18. P. J. LI, C. OHTSUKI, T. KOKUBO, K. NAKANISHI, N. SOGA and T. NAKAMURA, *J. Am. Ceram. Soc.* **75**(8) (1992) 2094.
19. I. M. O. KANGASNIEMI, E. VEDEL, J. DE BLICK-HOGERWORST, A. YLIURPO and K. DE GROOT, *J. Biomed. Mater. Res.* **27** (1993) 1225.
20. K. H. KARLSSON, K. FROBERG and T. RINGBOM, *J. Non-Cryst. Solids* **112** (1989) 69.
21. P. J. LI and F. P. ZHANG, *J. Non-Cryst. Solids* **119** (1990) 112.
22. P. J. LI, *J. Biomed. Mater. Res.* **28** (1994) 7.
23. J. P. ZHONG, G. P. LATORRE, D. C. GREENSPAN and L. L. HENCH, in ''Bioceramics 8'', edited by L. L. Hench, J. Wilson, and D. C. Greenspan (Elsevier Science, 1995) p. 489.
24. L. L. HENCH, in ''Bioceramics 9'', edited by T. Kokubo, T. Nakamura and F. Miyaji (Pergamon, 1996) 3.
25. L. CHOU, S. AL-BAZIE, D. COTTRELL, R. GIODANO and D. NATHASON, in ''Bioceramics 11'', edited by R. LeGeros and J. LeGeros (World Scientific, 1998) p. 265.
26. T. KOKUBO, H. KUSHITANI, S. SAKKA, T. KITSUGI and T. YAMAMURO, *J. Biomed. Mater. Res.* **24** (1990) 721.
27. A. E. CLARK, C. G. PANTANO and L. L. HENCH, *J. Am. Ceram. Soc.* **59**(1–2) (1976) 37.
28. D. C. GREENSPAN, J. P. ZHONG and G. P. LATORRE, in ''Bioceramics 7'', edited by Ö. H. Andersson, R. P. Happonen, A. YliUrpo (Butterworth-Heinemann, 1994) p. 55.
29. M. R. FILGUEIRAS, G. P. LATORRE and L. L. HENCH, *J. Biomed. Mat. Res.* **27** (1993) 445.
30. S. RADIN, P. DUCHEYNE, S. FALAIZE and A. HAMMOND, in ''Bioceramics 10'', edited by L. Sedel and C. Rey (Elsevier Science, 1997) p. 45.
31. J. P. ZHONG and D. C. GREENSPAN, Transactions of the 23rd Annu. Meeting of the Soc. for Biomater. (New Orleans, LA, 1997) p. 125.
32. W. BONFIELD and Z. B. LUKLINSKA, in ''The Bone-

Biomaterial Interface'', edited by J. E. Davies (University of Toronto, 1990) p. 89.
33. Y. MIAKE, T. YANAGISAWA, Y. YAJIMA, H. NOMA, N. YASUI and T. NONAMI, *J. Dent. Res.* **74**(11) (1995) 1756.
34. D. C. GREENSPAN, J. P. ZHONG, X. F. CHEN and G. P. LATORRE, in ''Bioceramics 10'', edited by L. Sedel and C. Rey (Elsevier Science, 1997) p. 391.
35. J. J. M. DAMEN and J. M. TEN CATE, *J. Dent. Res.* **71**(3) (1992) 453.
36. J. J. M. DAMEN and J. M. TEN CATE, *J. Dent. Res.* **68**(9) (1989) 1355.
37. F. S. KAPLAN, W. C. HAYES, T. M. KEAVENY, A. BOSKEY and J. P. IANNOTTI, in Orthopaedic Basic Science, edited by S. R. Simon (American Academy of Orthopaedic Surgeons, 1994) p. 127.
38. J. WILSON and S. B. LOW, *J. Appl. Biomater.* **3** (1992) 123.

Recevied 30 March 2000
and accepted 29 June 2001